Title

The Bartonella quintana Extracytoplasmic Function Sigma Factor RpoE Has a Role in Bacterial Adaptation to the Arthropod Vector Environment

Journal

Journal of Bacteriology, 195(11)

ISSN

0021-9193

Authors

Abromaitis, Stephanie
Koehler, Jane E

Publication Date

2013-06-01

DOI

10.1128/jb.01972-12

Peer reviewed

JB
Journals.ASM.org

The *Bartonella quintana* Extracytoplasmic Function Sigma Factor RpoE Has a Role in Bacterial Adaptation to the Arthropod Vector Environment

Stephanie Abromaitis,* Jane E. Koehler

Microbial Pathogenesis and Host Defense Program and Division of Infectious Diseases, Department of Medicine, University of California at San Francisco, San Francisco, California, USA

***Bartonella quintana* is a vector-borne bacterial pathogen that causes fatal disease in humans. During the infectious cycle, *B. quintana* transitions from the hemin-restricted human bloodstream to the hemin-rich body louse vector. Because extracytoplasmic function (ECF) sigma factors often regulate adaptation to environmental changes, we hypothesized that a previously unstudied *B. quintana* ECF sigma factor, RpoE, is involved in the transition from the human host to the body louse vector. The genomic context of *B. quintana rpoE* identified it as a member of the ECF15 family of sigma factors found only in alphaproteobacteria. ECF15 sigma factors are believed to be the master regulators of the general stress response in alphaproteobacteria. In this study, we examined the *B. quintana* RpoE response to two stressors that are encountered in the body louse vector environment, a decreased temperature and an increased hemin concentration. We determined that the expression of *rpoE* is significantly upregulated at the body louse (28°C) versus the human host (37°C) temperature. *rpoE* expression also was upregulated when *B. quintana* was exposed to high hemin concentrations. *In vitro* and *in vivo* analyses demonstrated that RpoE function is regulated by a mechanism involving the anti-sigma factor NepR and the response regulator PhyR. The Δ*rpoE* Δ*nepR* mutant strain of *B. quintana* established that RpoE-mediated transcription is important in mediating the tolerance of *B. quintana* to high hemin concentrations. We present the first analysis of an ECF15 sigma factor in a vector-borne human pathogen and conclude that RpoE has a role in the adaptation of *B. quintana* to the hemin-rich arthropod vector environment.**

The Gram-negative bacterial pathogen *Bartonella quintana* was first identified during World War I as the causative agent of trench fever, a 5-day relapsing fever (1). In the last 2 decades, there has been a resurgence of *B. quintana* infections, with the most severe illness occurring among immunocompromised individuals (2). *B. quintana* infection can cause relapsing fever, endocarditis, and vascular proliferative lesions (3). Vasculoproliferative *B. quintana* infection is usually progressive and can be fatal unless correctly diagnosed and treated with antibiotic therapy (4). Another manifestation of *B. quintana* infection is persistent bloodstream infection, which occurs in both immunocompromised and immunocompetent people (5, 6).

Bartonella is an arthropod vector-borne bacterium. The vector for *B. quintana* is the human body louse *Pediculus humanus humanus*. In a recent analysis, 33.3% of the body lice recovered from infested homeless individuals in California were PCR positive for *B. quintana*, underscoring the high prevalence of this potentially fatal bacterium in the human environment (7). *B. quintana* colonizes the louse alimentary tract and can attach to the apical surface of gut epithelial cells (8). The louse excretes *B. quintana* in its feces during feeding, and feces containing *B. quintana* are inoculated into the louse bite when the human scratches the bite. *B. quintana* forms a biofilm-like structure in the louse feces, allowing prolonged bacterial survival within the fecal environment (9).

During the infectious cycle, *B. quintana* alternates between two niches, the bloodstream of the human host (37°C) and the gut of the body louse vector (28°C) (10). To maintain the transmission cycle, *B. quintana* must survive and proliferate within these two different environments. The adaptive mechanisms utilized by *Bartonella* during the transition between the host and vector are unknown. In addition to temperature, a major environmental difference between the host and vector niches is the ambient hemin concentration; the bloodstream is severely hemin restricted, and the body louse gut is hemin rich. Hemin and hemoglobin are the only iron sources that *Bartonella* can utilize (11), making the acquisition and metabolism of these nutrients essential for *Bartonella* survival. However, hemin can produce reactive oxygen molecules that are potentially toxic (12). *Bartonella* is unique in its ability to survive exposure to hemin concentrations that are typically bactericidal (>1 mM) (11, 13, 14). For example, the growth of *Staphylococcus aureus* is severely limited in 10 to 20 μM hemin (15, 16) and the growth of *Neisseria meningitidis* is inhibited by ~0.2 mM hemin (17). *Bartonella* produces a family of hemin binding proteins (Hbp) that are responsive to temperature, hemin concentration, and oxidative stress (18, 19). Additionally, *Bartonella* contains a genomic locus that encodes hemin utilization (Hut) proteins involved in hemin sensing, degradation, and storage (20). It is believed that both Hbp and Hut proteins have a role in the unique ability of *Bartonella* to survive in a wide range of hemin concentrations (18–21).

Received 8 October 2012 **Accepted** 27 March 2013
Published ahead of print 5 April 2013
Address correspondence to Jane E. Koehler, jkoehler@medicine.ucsf.edu.
* Present address: Stephanie Abromaitis, Food and Drug Laboratory Branch, California Department of Public Health, Richmond, California, USA.
Supplemental material for this article may be found at http://dx.doi.org/10.1128/JB.01972-12.

doi:10.1128/JB.01972-12

Many bacteria adapt to environmental changes by expressing different sigma factors. Bacterial sigma factors mediate shifts in gene expression by conferring promoter recognition specification on RNA polymerase (22). Thus, the expression of different sigma factors allows a bacterium to coordinate the transcription of specific sets of genes as a regulon. On the basis of sequence homology, the *B. quintana* genome encodes four sigma factors (23), none of which have been studied. The four *B. quintana* sigma factors belong to the σ^{70} family: RpoD (σ^{70}, σ^{D}), RpoH1 (σ^{32}, σ^{H}), RpoH2 (σ^{32}, σ^{F}), and RpoE (σ^{24}, σ^{E}). *Bartonella* RpoE was annotated as SigH in the original genome sequence (23); however, in an earlier publication it was referred to as RpoE (24). We have adopted the RpoE nomenclature because, in general, sigma factors from Gram-negative bacteria are given the designation *rpo* (for RNA polymerase subunit), whereas sigma factors from Gram-positive bacteria are typically given the *sig* designation (25).

The *Bartonella* alternative sigma factor RpoE is annotated as an extracytoplasmic function (ECF) sigma factor. ECF sigma factors typically sense and respond to changes in the extracellular environment, including oxidative stress, misfolded proteins, and changes in temperature, pressure, or nutrient concentration (26, 27). The ECF sigma factor family is the largest and most divergent of the bacterial sigma factor families (25). Over 40 distinct groups of ECF sigma factors have been identified (28). By sequence homology and genomic context, *Bartonella* RpoE appears to be a member of the sigma factor group designated ECF15, which is found only in alphaproteobacteria (28). The ECF15 sigma factor mediates the general stress response (GSR) in alphaproteobacteria (29). The GSR allows bacteria to respond to a wide variety of stress conditions in a nonspecific manner (29). The ECF15 group is characterized by the conserved genomic context of the sigma factor, with an anti-sigma factor and a unique response regulator found in close proximity (28). The involvement of the ECF15-associated response regulator in the alphaproteobacterial GSR was first described in 2006, for *Methylobacterium extorquens* (30). Members of this newly recognized ECF15 sigma factor group have been studied subsequently in the nonpathogenic alphaproteobacteria *Bradyrhizobium* (31), *Sinorhizobium* (32), *Caulobacter* (33–35), and *Sphingomonas* (36, 37). In these organisms, the associated anti-sigma factor is named NepR, except for that of *Sinorhizobium*, which is called RsiA1 (32).

In the above-mentioned alphaproteobacteria, there is a response regulator found in close genomic proximity to the ECF15 sigma factor that functions as an anti-anti-sigma factor (28). The response regulator is named PhyR, corresponding to the name established in the initial studies in *Methylobacterium* (30, 38). PhyR response regulators contain an ECF sigma factor-like domain and function as an anti-anti-sigma factor by binding to the anti-sigma factor NepR, thus disrupting the NepR-RpoE interaction (33, 38). There is typically a sensor histidine kinase gene in close genomic proximity to the gene for either the ECF15 sigma factor or PhyR (29). It has been demonstrated in *Caulobacter* that the sensor histidine kinase (PhyK) phosphorylates the response regulator PhyR (35). Phosphorylation triggers the conformational change that allows PhyR to interact with NepR (33, 34). It also was shown that the putative histidine kinase in *Sphingomonas*, PhyP, is a phosphatase that functions to maintain PhyR in an unphosphorylated state (37).

The goals of this study were to identify the genomic components and functional interactions of the *B. quintana* ECF15 transcription regulatory system and to determine the role of RpoE-mediated transcription in the *B. quintana* infectious cycle. We demonstrated that the expression of the *B. quintana* sigma factor *rpoE* is significantly upregulated under low-temperature and high-hemin conditions that recapitulate the body louse environment. We further determined that RpoE-mediated transcription has a role in mediating *B. quintana* tolerance to toxic hemin concentrations. *B. quintana* RpoE is the first ECF15 group sigma factor found to be involved in adaptation to arthropod vector conditions; thus, our work has identified a novel adaptation of the alphaproteobacterial GSR ECF15 class of sigma factors. Additionally, our data provide the first detailed study of the role of an ECF15 sigma factor in a bacterium pathogenic to humans.

MATERIALS AND METHODS

Bacterial strains and growth conditions. Wild-type *B. quintana* strain JK31 was isolated from a *B. quintana*-infected individual (39). Low-passage *B. quintana* strains were used for all experiments. *B. quintana* strains from frozen stock were streaked onto fresh chocolate agar plates (40) and grown for 6 to 7 days in candle extinction jars at 35°C prior to passage and use in experiments. The liquid *Bartonella* medium used in some experiments, M199S, consists of M199 medium supplemented with 20% fetal bovine serum, glutamine, and sodium pyruvate (40). *Escherichia coli* strains were grown at 37°C on Luria-Bertani medium. When required, kanamycin was used at a final concentration of 50 $\mu g\ ml^{-1}$, ampicillin was used at 100 $\mu g\ ml^{-1}$, cefazolin was used at 20 $\mu g\ ml^{-1}$, and nalidixic acid was used at 2 $\mu g\ ml^{-1}$. For *sacB* negative selection, a sterile filtered sucrose solution was added to chocolate agar to give a final concentration of 5%. The strains and plasmids used in this study are listed in Table 1.

***Bartonella* RNA, cDNA, and genomic DNA preparation.** For RNA isolation, *B. quintana* were harvested from confluent plates into 1 ml stop solution (M199, 45% ethanol, 5% water-saturated phenol) to prevent RNA degradation (41). Bacteria were then pelleted by centrifugation at 4,000 × *g* at 4°C. The bacterial pellet was stored at −80°C until RNA isolation. Bacterial cells were lysed by incubation in fresh lysozyme (0.4 $mg\ ml^{-1}$) in 10 mM Tris and 1 mM EDTA for 5 min at room temperature. The RNA was extracted with TRIzol reagent (Invitrogen, Carlsbad, CA) in accordance with the manufacturer's instructions. Total RNA was RQ1 DNase (Promega, Madison, WI) treated for 2 h and then further purified with the RNeasy Mini Kit (Qiagen, Valencia, CA). A second RQ1 DNase treatment and RNA cleanup were performed to ensure complete DNA removal. cDNA was generated from 0.5 μg of total RNA with random hexamer primers (Invitrogen) and SuperScript III (Invitrogen) by following the manufacturer's instructions. Reverse transcription reactions without Superscript III were performed as negative controls and to evaluate DNase treatment efficiency. *B. quintana* genomic DNA was isolated with Qiagen Puregene Core Kit B by following the manufacturer's instructions.

Quantitative analysis of *B. quintana* gene expression. The relative abundance of specific mRNA sequences was ascertained by reverse transcriptase quantitative PCR (RT-qPCR) with an MX3000P machine (Stratagene/Agilent Technologies, Santa Clara, CA). cDNA was diluted 1:10 for use in reaction mixtures. The reaction mixture included 10 μl of SYBR Fast qPCR master mix (Kapa Biosystems, Woburn, MA), 0.4 μl of ROX low (Kapa Biosystems), 7.6 μl of template, and 2 μl of 1 pmol μl^{-1} primer. The reaction conditions were 95°C for 10 min and 40 cycles of 95°C for 15 s and 60°C for 60 s, with the standard dissociation protocol. Threshold fluorescence was determined during the geometric phase of logarithmic gene amplification; from this the quantification cycle (C_q) was set. Standard curves for each primer set were generated by plotting log genomic DNA versus the C_q. These plots were used to ensure that equivalent reaction efficiency was obtained with all primer sets. The primers used are listed in Table S1 in the supplemental material. The relative levels of gene transcripts in samples were determined by converting the transcript level into a genomic copy number by using standard curves. This

TABLE 1 Bacterial strains and plasmids used in this study

Strain or plasmid	Description	Source or reference
B. quintana strains		
JK31 (wild type)	Human isolate from a patient with bacillary angiomatosis	39
Δ*rpoE* Δ*nepR* mutant	JK31 background with *rpoE* and *nepR* deleted	This study
*nepR** mutant	JK31 background containing plasmid pANT4Δ*gfp-nepR*	This study
E. coli strains		
TOP10	Cloning strain	Invitrogen
BL21(DE3)	Expression strain	Invitrogen
S17-1	Strain for biparental conjugation	71
Plasmids		
pCR2.1-TOPO-TA	Cloning vector	Invitrogen
pET-22b(+)	Vector used for expression of *gfp* in *E. coli*	Novagen
pET-28a(+)	Vector used for expression of *B. quintana rpoE* in *E. coli*	Novagen
pMAL-c2x	Vector used for expression of *B. quintana nepR* and *phyR* in *E. coli*	New England Biolabs
pET22-GFP-FLAG	pET-22b(+) vector containing *gfp* with a C-terminal FLAG tag	This study
pET28-His-RpoE	pET-28a(+) vector containing *rpoE* with an N-terminal His tag	This study
pMAL-MBP-NepR	pMAL-c2x vector containing *nepR* with an N-terminal MBP tag	This study
pMAL-MBP-PhyR	pMAL-c2x vector containing *phyR* with an N-terminal MBP tag	This study
pANT3	Vector containing *gfp* without a promoter	43
pANT3-pRpoE-GFP	pANT3 vector containing the *rpoE* operon promoter region fused to GFP	This study
pANT3-pPhyR-GFP	pANT3 vector containing the *phyR* operon promoter region fused to GFP	This study
pANT4	Vector containing GFP under the control of the P_{tac} promoter	43
pANT4Δ*gfp*	pANT4 vector in which *gfp* has been deleted	This study
pANT4Δ*gfp-nepR*-FLAG	pANT4Δ*gfp* vector containing *nepR* with a C-terminal FLAG tag under the control of the P_{tac} promoter	This study

value was divided by the genomic copy number of the constitutively expressed *B. quintana* reference gene *purA* (adenylosuccinate synthetase) to obtain a relative level of transcription for each gene. Data from three independent experiments were used for statistical analysis by Student's *t* test and to determine average gene transcription values.

Mapping of the transcriptional start site (TSS) by 5′ random amplification of cDNA ends (RACE). 5′ RACE was performed as described by Frohman et al. (42). RNA was purified as described above. cDNA was generated from 5 μg of RNA, but gene-specific primers (GSP1) were used in place of random hexamers. All of the primers used for 5′ RACE are listed in Table S1 in the supplemental material. cDNA was treated with RNase H (Invitrogen) and then purified with Qiagen PCR purification columns. A poly(A) tail was added to the 3′ end of the purified cDNA with terminal transferase (Roche, Indianapolis, IN). Tailed cDNA was used as the template for PCR with the GSP2 primer and the oligo(dT) anchor primer. This PCR product was then used as the template for a nested PCR with the GSP3 primer and the PCR anchor primer. Products were separated on 2% agarose gels, and bands of interest were excised and cloned into the pCR2.1-TOPO vector (Invitrogen). Resultant bacterial colonies containing plasmids with the appropriate insert size were selected, and the insert was sequenced.

Overproduction and purification of *B. quintana* proteins from *E. coli*. GFP with a C-terminal FLAG tag was PCR amplified from the pANT4 vector (43) with the primers listed in Table S1 in the supplemental material. The PCR product was ligated into the pCR2.1-TOPO-TA vector, which was then digested with XbaI and XhoI, and the insert was ligated into the pET-22b(+) vector (Novagen, Madison, WI). *B. quintana* wild-type strain JK31 genomic DNA was used as the template for PCR amplification of *rpoE* (BQ10960), *nepR* (BQ10970), and *phyR* (BQ10980); the primers used are listed in Table S1. The PCR products were ligated into the pCR2.1-TOPO-TA vector (Invitrogen). The *rpoE*-containing TOPO-TA vector was digested with NdeI and EcoRI. The digestion product was ligated into the pET-28a(+) vector (Novagen) to generate RpoE with an N-terminal 6×His tag. The *nepR*-containing TOPO-TA vector was digested with HindIII and EcoRI. The digestion product was ligated into the pMAL-c2x vector (New England BioLabs, Ipswich, MA) to generate NepR with an N-terminal maltose binding protein (MBP) tag. The *phyR*-containing TOPO-TA vector was digested with EcoRI and PstI. The digestion product was ligated into the pMAL-c2x vector to generate PhyR with an N-terminal MBP tag. All vectors were transformed into *E. coli* BL21(DE3).

For recombinant protein expression and purification, overnight cultures were diluted 1:40 and grown with shaking at 37°C for 1.5 h. Protein expression was induced by the addition of isopropyl-β-D-thiogalactopyranoside (IPTG) at a final concentration of 0.2 mM. Following induction, cells were grown at 30°C for 3 h, harvested, and stored at −20°C until purification.

To purify His-tagged RpoE and MBP-tagged NepR or PhyR, the cell pellet from 1 liter of bacteria was suspended in 20 ml of 4°C-chilled Novagen His-Bind buffer supplemented with 100 μg ml^{-1} lysozyme and protease inhibitor cocktail [PIC; 100× PIC is 20 mM 4-(2-aminoethyl) benzenesulfonyl fluoride hydrochloride, 1 mg ml^{-1} leupeptin, 0.36 mg ml^{-1} E-64 protease inhibitor, and 5.6 mg ml^{-1} benzamidine] or in 18 ml 4°C-chilled MBP buffer (20 mM Tris HCl [pH 7.4], 200 mM NaCl, 1 mM EDTA, 1 mM sodium azide) supplemented with 100 μg ml^{-1} lysozyme and PIC. The resuspended pellet was incubated for 15 min on ice, and 0.1% Sarkosyl was added. Cells were lysed by sonication and then centrifuged for 20 min at 9,000 × *g* at 4°C. The supernatant was passed through a 0.2-μm filter and then applied to a Novagen His-Bind column or a column containing Amylose Resin (New England BioLabs). Proteins were purified in accordance with the manufacturer's instructions. Following purification, elution buffer was exchanged by dialysis against 20 mM Tris HCl (pH 8.0) containing 10% glycerol.

To purify FLAG-tagged green fluorescent protein (GFP), the cell pellet from 600 ml of bacteria was suspended in 5 ml of 4°C-chilled CelLytic B solution (Sigma, St. Louis, MO) supplemented with 100 μg ml^{-1} lysozyme and PIC. Cells were incubated in this solution for 10 min at 4°C with vigorous shaking and then centrifuged for 10 min at 10,000 × *g* at 4°C. The supernatant was passed through a 0.2-μm filter and then loaded

onto a column containing anti-FLAG M2 affinity gel resin (Sigma). FLAG-tagged protein was purified in accordance with the manufacturer's instructions. Following purification, elution buffer was exchanged by dialysis against 20 mM Tris HCl (pH 8.0) containing 10% glycerol.

***In vitro* transcription analysis.** Overlap PCR (43) was used to generate fusion products of *gfp* with the *rpoE* operon promoter and the *phyR* operon promoter. The promoters were amplified from *B. quintana* genomic DNA with the primers listed in Table S1 in the supplemental material. *gfp* was amplified from the pANT4 plasmid (43) with the primers listed in Table S1. PCR products were purified and ligated by overlap PCR. The resultant promoter-*gfp* fusion products were gel extracted and ligated into pCR2.1-TOPO-TA. The TOPO vectors containing the promoter-*gfp* fusion products were digested with NotI and BamHI, and the digestion products were ligated into a NotI- and BamHI-digested pANT3 vector (43). The resultant recombinant plasmids and pANT3, which contains promoterless *gfp*, were used as the templates for *in vitro* transcription assays.

Ten pmol of purified recombinant RpoE protein, with or without 20 pmol of purified recombinant NepR, was incubated for 30 min at 32°C in transcription buffer (40 mM Tris [pH 7.9], 10 mM $MgCl_2$, 0.6 mM EDTA, 0.4 mM potassium phosphate, 1.5 mM dithiothreitol [DTT], 0.25 mg ml^{-1} bovine serum albumin, 20% glycerol) (44, 45). Next, 1.8 pmol of *E. coli* core RNA polymerase (Epicentre, Madison, WI) was added and the reaction mixtures were incubated for 10 min at 32°C. Following that incubation, 40 U of RNasin (Promega) and 50 fmol of template DNA (purified plasmid containing the promoter-*gfp* fusion or purified pANT3) were added to each reaction mixture. The reaction mixtures were incubated for an additional 10 min at 32°C to allow RNA polymerase binding to template DNA. Transcription was initiated by the addition of 300 μM nucleoside triphosphates. After 2 min at 32°C, 50 μg ml^{-1} heparin was added to prevent reinitiation. Reaction mixtures were incubated for a final 30 min at 32°C.

Following transcription, reaction mixtures were treated with 5 U of RQ1 DNase (Promega) for 4 h at 37°C. RNA was then purified with the Qiagen RNeasy Mini Kit and eluted in a final volume of 40 μl. Reverse transcription of 2 μl of RNA was carried out as described above. GFP transcription was quantified by RT-qPCR as described above, with the primers listed in Table S1 in the supplemental material. cDNA was diluted 1:200 prior to use in RT-qPCR. The relative level of transcription was determined by converting the transcript level into a copy number by using a standard curve. This value was then compared to reaction mixtures containing the plasmid encoding a promoterless *gfp* gene (pANT3) as the template. Data from three independent experiments were used for statistical analysis by Student's *t* test and to determine average gene transcription values.

Generation of *B. quintana* Δ*rpoE* Δ*nepR* null mutant and *nepR* overexpression strains. The Δ*rpoE* Δ*nepR* mutant strain used in this study was generated by targeted allelic replacement. The genomic regions upstream and downstream of the *rpoE* and *nepR* genes were amplified with the primers listed in Table S1 in the supplemental material. These two products were then used as the template in an overlap PCR that generated a genomic fragment with an in-frame deletion of the coding sequence of *rpoE* and *nepR*. The Δ*rpoE* Δ*nepR* mutant deletion strain was constructed by a previously described two-step *sacB*-mediated mutagenesis method (46).

NepR was amplified from wild-type *B. quintana* genomic DNA to generate a NepR overexpression strain with the primers listed in Table S1 in the supplemental material. An N-terminal Shine-Dalgarno sequence and a C-terminal FLAG tag were added during PCR amplification. The PCR products were ligated into pCR2.1-TOPO-TA (Invitrogen). The TOPO-TA vector was then digested with SphI and BamHI, and the digestion product was ligated into the SphI- and BamHI-digested pANT4Δ*gfp* vector. The resultant vector was transformed into *E. coli* S17-1, and biparental conjugation with wild-type *B. quintana* was performed. Kan^r colonies were screened by immunoblotting with anti-FLAG antibody (Sigma) to confirm the expression of the recombinant protein.

***B. quintana* RpoE protein binding analyses.** For analysis of binding interactions, 250 pmol of purified 6×His-RpoE was incubated with 500 pmol of purified MBP-NepR or 500 pmol of purified GFP-FLAG for 10 min at room temperature and then for 20 min at 4°C to allow interaction. When PhyR was analyzed, 250 pmol of purified 6×His-RpoE was incubated with 500 pmol of purified MBP-NepR, with or without 500 pmol MBP-PhyR, for 30 min at room temperature to allow interaction. When included for phosphorylation, lithium potassium acetyl phosphate (Sigma) was present at a final concentration of 25 mM (47). Protein interactions were performed in interaction buffer (Novagen His-Bind buffer supplemented with 50 mM KCl, 5 mM $MgCl_2$, and 1 mM DTT). Following incubation, 200 μl of charged His-Bind resin was added and the reaction mixtures were incubated for 30 min. Unbound protein was removed in accordance with the manufacturer's protocol for small-scale purification. Eluted proteins were assessed by sodium dodecyl sulfate polyacrylamide gel electrophoresis (SDS-PAGE), followed by silver staining.

Quantification of *B. quintana* tolerance during exposure to high hemin concentrations. To evaluate the Δ*rpoE* Δ*nepR* mutant strain for a growth defect, *B. quintana* wild-type or Δ*rpoE* Δ*nepR* mutant bacteria were grown on chocolate agar plates and the growth of the two strains was compared by plating serial dilutions. The *B. quintana* strains were harvested, pelleted, and washed three times in phosphate-buffered saline (PBS), and the bacterial pellet was resuspended in M199S medium. to a final optical density at 600 nm (OD_{600}) of 1. Serial dilutions of the bacterial suspension were prepared, and 8 μl of each dilution were spotted onto chocolate agar plates. Duplicate sets of plates were prepared and grown in candle extinction jars, one set at 37°C and the other at 28°C.

To evaluate the tolerance of *B. quintana* to a high hemin concentration (10 mM), the *B. quintana* wild-type and isogenic mutant (Δ*rpoE* Δ*nepR*) strains were plated on minimal medium plates that do not support *Bartonella* growth, with hemin supplied via saturated disks placed on the agar. This assay was selected for our analysis of bacterial hemin tolerance on solid medium because the more restrictive growth conditions allowed us to observe hemin-specific growth phenotypes that could not be observed on permissive chocolate agar medium. Minimal medium plates were prepared with *Brucella* broth (BD Biosciences, San Diego, CA) and Bacto agar (BD Biosciences) (18). An 80-μl volume of a *B. quintana* suspension with an OD_{600} of 1 was spread onto each plate. Dilutions of each bacterial suspension also were plated on chocolate agar to enumerate CFU and to ensure that an equivalent number of each *B. quintana* strain was used.

For hemin solution preparation, hemin chloride powder (Sigma) was washed with 0.1 N HCl three times to remove any iron contamination. The hemin chloride was then suspended in 0.1 N NaOH and filtered to remove hemin chloride that had not solubilized. The concentration of the resultant solution was determined by measuring the OD_{572}; a 1 mM hemin solution has an OD_{572} of 5.5 (48). The hemin solution was then adjusted to the appropriate concentration, and the pH was adjusted to the pH of M199S medium (~8.5). Hemin solutions were stored in the dark at −20°C and used within 1 week of preparation. A sterile 0.7-mm Whatman paper disk was placed on the center of each plate, and 8 μl of hemin solution or M199 control medium was applied to the disk. Plates were grown in candle extinction jars at 37°C for 14 days or at 28°C for 28 days. The distance from the edge of the disk to the leading edge of the zone of bacterial growth was measured. Three plates were analyzed per strain in each experiment, and statistical analysis by Student's *t* test was based on averaged data from three independent experiments.

A second method used to analyze *B. quintana* tolerance to exposure to high hemin concentrations was based on the hemin tolerance assay described by Roden et al. (21). For this assay, wild-type or Δ*rpoE* Δ*nepR* mutant *B. quintana* was grown on chocolate agar plates at 37 or 28°C. The bacteria were harvested, pelleted, and washed three times in PBS. The bacterial pellet was resuspended in M199S medium to a final OD_{600} of 1.

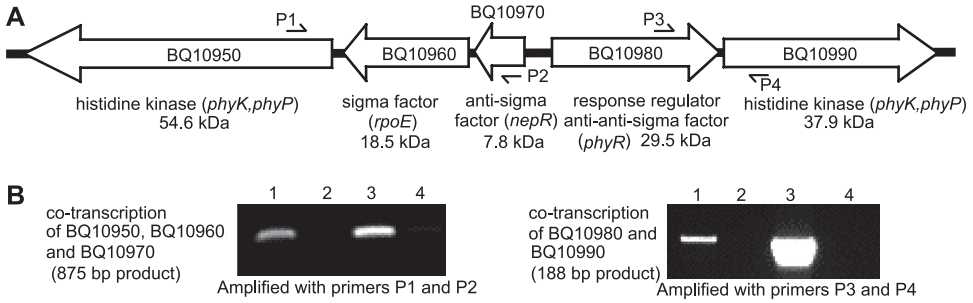

FIG 1 *B. quintana* RpoE (BQ10960) is an alphaproteobacterial ECF15 sigma factor. (A) The genomic context of the gene for RpoE (BQ10960) is shown. On the basis of homology, the gene name(s), predicted function, and predicted molecular mass are indicated below each open reading frame. (B) The operon structure was determined by RT-PCR analysis of cDNA amplified from *B. quintana* with the primers (P1 to P4) depicted as small arrows in panel A. cDNA was generated from *B. quintana* RNA with (lane 1) or without (lane 2) RT, from genomic DNA with RT (lane 3), and with RT with H_2O as the template (lane 4).

A 20-μl volume of 500, 250, or 50 mM hemin was added to 1 ml of the bacterial suspension to generate a solution with a final hemin concentration of 10, 5, or 1 mM. All of the hemin solutions were pH balanced prior to addition to the bacterial suspension, and a pH-balanced control solution was added to bacteria for the 0 mM control cultures. Bacteria were grown for 24 h at 37 or 28°C. After incubation, the bacteria were pelleted and washed three times with M199S medium. Following the final wash, the bacteria were resuspended in 1 ml of M199S medium. Serial dilutions of the bacterial suspension were prepared and plated to enumerate the CFU. Percent survival was determined by comparing the *B. quintana* grown in hemin-containing medium with the *B. quintana* grown in the 0 mM hemin medium. Data from three independent experiments were used for statistical analysis by Student's *t* test.

Quantification and visualization of hemin binding by *B. quintana*. To quantify hemin binding by *B. quintana* bacteria, a modification of the hemin binding assay described by Minnick et al. (49) and Roden et al. (21) was used. Bacteria were harvested from chocolate agar plates grown at 37 or 28°C and then washed three times with PBS. The pelleted bacteria were then resuspended in PBS and adjusted to an OD_{600} of 1. Hemin was added to the bacterial suspensions, and the mixture was incubated for 1 h at 37 or 28°C. During incubation, bacterial suspensions were mixed every 15 min. Following the 1 h of incubation, cells were pelleted by centrifugation for 2 min at 16,000 × *g*. The supernatant was removed and centrifuged again to remove any remaining bacteria. The amount of hemin present after centrifugation was quantified by measuring the absorbance of the supernatant at 400 nm (21, 49). The amount of hemin bound by *B. quintana* was calculated and compared to that in an identical control reaction mixture without bacteria. A saturation plot for hemin binding was generated. Data from three independent experiments were used for statistical analysis by Student's *t* test and for nonlinear regression analysis to determine the association constant (K_a) and maximum binding (B_{max}). Nonlinear regression analysis was done with GraphPad Prism software.

To visually evaluate hemin binding, *B. quintana* strains were incubated in a 1 mM hemin solution for 1 h as described above. Following incubation, the bacteria were pelleted and washed three times with PBS. Control assays were performed without bacteria. The washed bacterial pellet was resuspended in 100 μl CelLytic B cell lysis solution (Sigma) and incubated for 15 min at room temperature. Serial 1:4 dilutions of the bacteria were prepared, and 4 μl of each dilution was spotted onto a nitrocellulose membrane. The membrane was dried, and hemin was then visualized by the addition of luminol-based chemiluminescence reagent and film exposure.

RESULTS

The homology and genomic context of *B. quintana* RpoE (BQ10960) define it as a member of the ECF15 sigma factor family. From our results and on the basis of the genomic context, the *B. quintana* BQ10960 protein (RpoE) is an ECF sigma factor and a member of the ECF15 group (Fig. 1A) (28). ECF15 sigma factors are cotranscribed with a small, soluble anti-sigma factor that lacks sequence homology to other RpoE anti-sigma factors (28). BQ10970 (Fig. 1A) is a 67-amino-acid protein with no predicted signal sequence or transmembrane domains, and it lacks homology to any proteins of known function. The small size (7.8 kDa), amino acid sequence, and genomic placement of BQ10970 suggest that it is an anti-sigma factor with functional homology to the NepR proteins identified for other alphaproteobacteria. PhyR, a response regulator that functions as an anti-anti-sigma factor, is typically found in close proximity to ECF15 sigma factors (28). We determined that BQ10980 is a putative response regulator with a high degree of homology to the four previously studied PhyR proteins (see Fig. S1 in the supplemental material) (31–33, 35, 38). BQ10980 has a C-terminal receiver domain and an N-terminal domain that has sequence similarity to ECF15 sigma factors; this domain structure is found in all of the PhyR response regulators studied (28). Additionally, previous genomic analysis of alphaproteobacteria performed by Starón and Mascher identified *Bartonella* species as containing a potential *phyR* locus with an associated ECF15 sigma factor and a NepR anti-sigma factor (29).

Frequently, one or more histidine kinase-encoding genes are found in the direct vicinity of the gene for an ECF15 sigma factor (28). The sequences and structures of histidine kinase-encoding genes in genomic proximity to ECF15 sigma factor-encoding genes are highly variable (28). The *B. quintana* genome contains a gene that encodes a putative histidine kinase (BQ10950) upstream of *rpoE* (Fig. 1A). We also identified a histidine kinase (BQ10990) gene that is downstream of that for the *B. quintana* response regulator (BQ10980) (Fig. 1A). BQ10950 is predicted to be periplasmic, whereas BQ10990 is predicted to be cytoplasmic. We found that both *B. quintana* histidine kinases have structural homology to *Caulobacter* PhyK and *Sphingomonas* PhyP. Structural analysis was performed with the SMART database (http://smart.embl-heidelberg.de/). The presence of two histidine kinase genes in close genomic proximity to the gene for *B. quintana* RpoE is unique among the ECF15 family sigma factors studied (31–33, 35, 37, 38). We used RT-PCR to define the structure of the *rpoE* operon and the BQ10980 (*phyR*) operon (Fig. 1B). As predicted, the genes for BQ10950, BQ10960 (*rpoE*), and BQ10970 (*nepR*) are cotranscribed as an operon; similarly, the genes for BQ10980 (*phyR*) and BQ10990 are cotranscribed as an operon (Fig. 1B).

Expression of *rpoE* is significantly upregulated in *B. quintana* after exposure to vector-specific conditions of low temperature (28°C) or high hemin concentrations. Because *B. quintana*

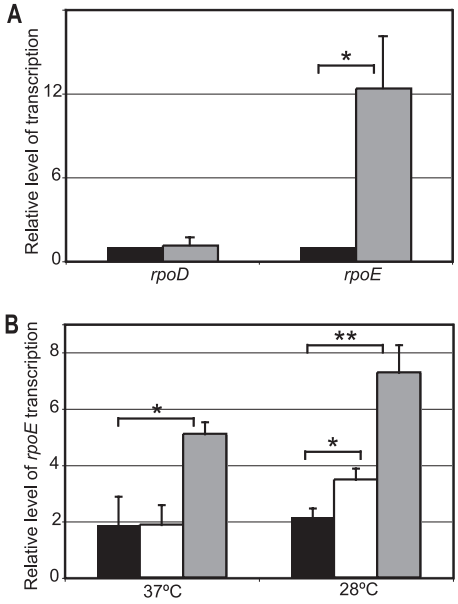

FIG 2 Transcription of *B. quintana rpoE* is increased at 28°C and in response to high hemin concentrations. (A) Relative *rpoD* or *rpoE* transcript levels in bacteria grown on chocolate agar plates at 37°C (black) or 28°C (gray) normalized to the constitutively expressed *B. quintana* reference gene *purA*. The 37°C values were set to 1 for comparison. (B) Relative *rpoE* transcript levels in bacteria grown for 24 h at 37 or 28°C in M199S medium supplemented with 0 mM (black), 1 mM (white), or 5 mM (gray) hemin. Transcript levels were normalized to *B. quintana purA*. Error bars indicate standard errors of the means. *, $P < 0.05$; **, $P < 0.01$ (Student's *t* test).

lives in two very different environments, the body louse vector and the human host, we sought to determine if RpoE is involved in directing bacterial transcription in these two environments. The expression of the alternative sigma factor gene *rpoE* and the housekeeping sigma factor gene *rpoD* was analyzed by RT-qPCR in bacteria grown at a temperature corresponding to the louse vector (28°C) or the human host (37°C), with two different growth media: solid chocolate agar and M199S liquid medium.

There was no significant difference in *rpoD* transcription at the two temperatures (Fig. 2A). However, the transcription of *rpoE* was significantly upregulated at 28°C compared with that at 37°C on solid chocolate agar (Fig. 2A). This suggested that RpoE is involved in directing transcription after exposure to the body louse temperature of 28°C. Interestingly, we observed a difference in the upregulation of *rpoE* at 28°C versus 37°C, depending on the medium type. Growth of *B. quintana* in M199S liquid medium without added hemin demonstrated no significant difference between the levels of *rpoE* expression at 28 and 37°C (Fig. 2B), in contrast to the significant upregulation of *rpoE* observed on solid chocolate agar medium at 28°C compared with 37°C (Fig. 2A). These two complex, undefined medium types are very different in composition and have different abilities to support *B. quintana* growth. This suggests that M199S medium (which has a bovine serum component) could present unique stressors that trigger the *Bartonella* GSR at 37°C, thus increasing the basal level of *rpoE* transcription and abrogating the difference between 28 and 37°C observed on solid agar.

When *B. quintana* colonizes the alimentary tract of the body louse, the bacterium is exposed to potentially toxic concentrations of hemin following the ingestion of a blood meal by the body louse (50). We therefore tested if *rpoE* transcription is responsive to changes in the hemin concentration. *B. quintana* was grown in M199S liquid medium supplemented with 0, 1, or 5 mM hemin for 24 h at 37 or 28°C, and *rpoE* transcription was quantified (Fig. 2B). In M199S medium, the transcription of *rpoE* was further upregulated in response to an increased hemin concentration (Fig. 2B), suggesting that RpoE has a role in the adaptation of *B. quintana* to life within the hemin-rich body louse gut. These data demonstrated that *rpoE* is highly transcribed under conditions mimicking those found in the body louse vector.

***B. quintana* RpoE positively regulates the transcription of the *rpoE* and *phyR* operons.** Many ECF sigma factors positively regulate their own transcription, which creates a positive feedback loop and amplification of the sigma factor-directed transcriptional changes (25). To determine if *B. quintana* RpoE positively regulates its own transcription, we first identified the TSS of the *rpoE* operon by 5′ RACE (Fig. 3A). We then performed *in vitro* transcription analysis by using the upstream region identified as the *rpoE* operon promoter fused to a promoterless GFP gene. When purified recombinant RpoE protein was added to *E. coli* RNA polymerase holoenzyme, significantly more *gfp* was transcribed than in the absence of RpoE ($P < 0.05$) (Fig. 3B). From these data, we concluded that RpoE directs the transcription of the *rpoE* operon. In *Bradyrhizobium* and *Caulobacter*, the transcription of *phyR* is positively regulated by the ECF15 sigma factor (31, 33). To test if the *B. quintana phyR* operon is similarly RpoE responsive, we first identified the TSS of the *phyR* operon by 5′ RACE (Fig. 3A). Next, *in vitro* transcription analysis was performed, which demonstrated that *B. quintana* RpoE directs the transcription of the *phyR* operon (Fig. 3C).

A comparison of the identified *B. quintana* ECF15 promoter consensus with the three ECF15 promoters that have been experimentally verified in other alphaproteobacteria is shown in Fig. 3D (31, 38, 51). The canonical motif of ECF15 sigma factor promoters is AAC-N_{17-18}-GTT (28). In our analysis of the *B. quintana rpoE* operon and the *phyR* operon, the −35 promoter elements we identified contained the AAC motif present in the canonical motif of ECF15 sigma factor promoters (28) (Fig. 3D). However, the −10 elements we identified lack a G residue associated with the TT motif. A secondary TSS was identified for the *phyR* operon. This secondary site was located 137 bp upstream of the ATG codon and yielded the −10 element CCATAT and the −35 element TTCATT. The identified −10 and −35 elements for this secondary TSS did not have any homology to either the −35 or the −10 consensus element of the ECF15 sigma factor (whereas the other *phyR* binding site had homology to the canonical −35 binding consensus), suggesting that this secondary *phyR* promoter functions independently of *rpoE*. To test for RpoE-independent transcription of the *phyR* operon, we sought to generate a strain of *B. quintana* in which *rpoE* is deleted. We were unable to delete only *rpoE* from the *B. quintana* genome, despite numerous attempts. However, simultaneous deletion of *rpoE* and *nepR* produced viable mutant bacteria. RT-qPCR was used to determine if *phyR* was transcribed in the Δ*rpoE* Δ*nepR* mutant strain. In the Δ*rpoE* Δ*nepR* mutant strain, *phyR* was transcribed; however, the level of transcription was significantly lower ($P \leq 0.01$) than that observed in wild-type *B. quintana* (Fig. 4). This result confirmed the presence of an RpoE-independent promoter.

The protein BQ10970, a NepR homolog, is the anti-sigma factor for *B. quintana* RpoE. RT-PCR analysis demonstrated that

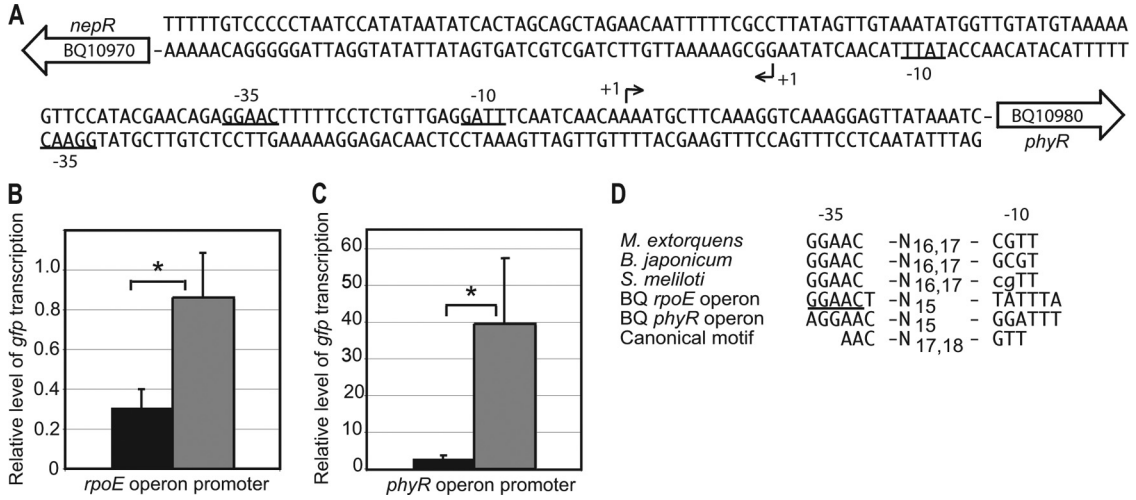

FIG 3 *B. quintana* RpoE positively regulates the transcription of the *rpoE* operon and the *phyR* operon. (A) The TSS of the *rpoE* operon and that of the *phyR* operon were determined by 5′ RACE. Each TSS is marked by an arrow. The −10 and −35 elements for each promoter are underlined. The initial gene in each operon is depicted as an open arrow with the open reading frame name. (B, C) Relative *gfp* transcript level produced in *in vitro* transcription assays containing *E. coli* core RNA polymerase without RpoE (black) or with RpoE (gray). The ratio of transcript produced with a plasmid containing *gfp* fused to the *rpoE* operon (B) or *phyR* operon (C) promoter versus a plasmid containing *gfp* without a promoter is shown. Error bars indicate standard errors of the means. *, $P < 0.05$ (Student's *t* test). (D) The −10 and −35 elements identified by 5′ RACE show homology to proposed ECF15 sigma factor consensus sequences of other alphaproteobacterial genera. The region of strong homology in the −35 element of each *B. quintana* (BQ) promoter is underlined.

rpoE is in an operon with the genes for BQ10950 and BQ10970 (Fig. 1). The small size and genomic context of BQ10970 suggested that it is an anti-sigma factor. In other alphaproteobacteria, the ECF15 sigma factor directly binds an anti-sigma factor, NepR. This binding sterically inhibits the interaction between the RNA polymerase core and the sigma factor (31, 32, 35, 37, 38). We tested for a direct interaction between *B. quintana* RpoE and BQ10970 with purified, recombinant, tagged versions of BQ10970, the putative anti-sigma factor, and RpoE. Purified 6×His-tagged RpoE was incubated with purified MBP-BQ10970 or the control protein GFP-FLAG. MBP-BQ10970 coeluted with 6×His-RpoE (Fig. 5), which demonstrated that BQ10970 binds directly to RpoE and likely is a NepR anti-sigma factor for *B. quintana* RpoE.

To further establish that BQ10970 functions as an anti-sigma factor, *in vitro* transcription analysis was performed with the *rpoE* operon promoter-*gfp* fusion construct described above. The addition of purified MBP-BQ10970 significantly reduced the RpoE-mediated transcription of *gfp* ($P < 0.05$) (Fig. 6A). The *phyR* operon promoter-*gfp* fusion construct also was analyzed by this assay. Similar to what was observed for the *rpoE* operon, the addition of BQ10970 significantly reduced the RpoE-mediated transcription of *gfp* ($P < 0.05$) from the *phyR* promoter operon construct (Fig. 6B). Additionally, when BQ10970 was overexpressed

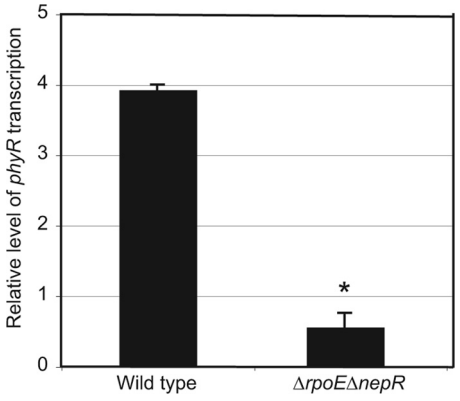

FIG 4 Transcription of *phyR* is significantly decreased in the *B. quintana* Δ*rpoE* Δ*nepR* mutant strain, but *phyR* transcript is still present. The presence of *phyR* transcript in the Δ*rpoE* Δ*nepR* mutant strain demonstrates that *phyR* is transcribed in both an RpoE-independent and an RpoE-dependent manner. The transcript amount was normalized to the constitutively expressed *B. quintana* reference gene *purA*. Error bars indicate standard errors of the means. *, $P \leq 0.01$ (Student's *t* test) compared to wild-type *B. quintana*.

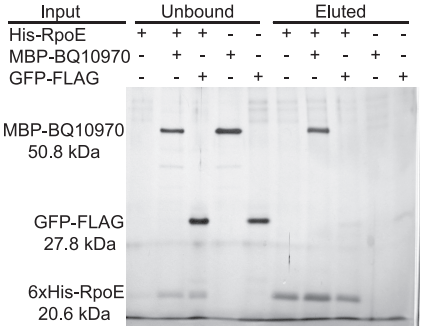

FIG 5 *B. quintana* RpoE binds directly to the *nepR* homolog BQ10970. Purified 6×His-RpoE (250 pmol) was incubated with 500 pmol of purified MBP-BQ10970 or 500 pmol of purified GFP-FLAG. The protein mixture was then applied to Ni-nitrilotriacetic acid resin. The resin was washed to remove unbound proteins, and RpoE and any interacting proteins were eluted with Novagen Elute buffer. The unbound and eluted proteins were separated by SDS-PAGE, and the gel was silver stained. MBP-BQ10970 coeluted with His-RpoE, but GFP-FLAG did not. Control assays with His-RpoE, MBP-BQ10970, and GFP-FLAG alone were also included. The molecular mass of each protein is indicated below the gene construct name.

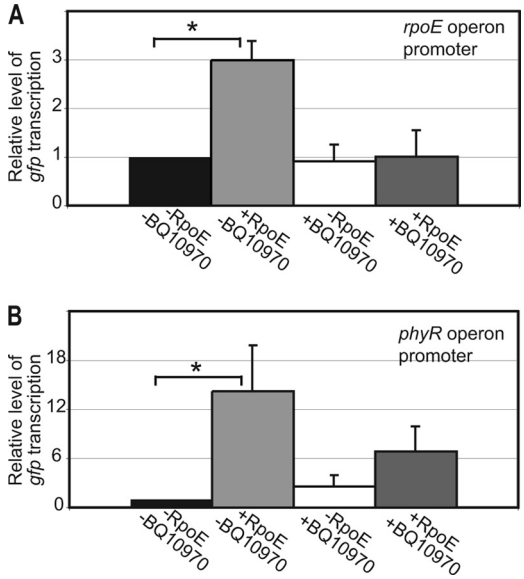

FIG 6 BQ10970 functions as the NepR anti-sigma factor for *B. quintana* RpoE. The relative *gfp* transcript levels produced in *in vitro* transcription assays with the *rpoE* operon promoter-*gfp* fusion construct (A) and the *phyR* operon promoter-*gfp* fusion construct (B) as the templates are shown. Assays included *E. coli* core RNA polymerase with (+RpoE) or without (−RpoE) purified recombinant *B. quintana* RpoE, with (+BQ10970) or without (−BQ10970) purified recombinant BQ10970. The ratio of the transcript produced from a plasmid containing *gfp* fused to the *rpoE* operon promoter or *phyR* operon promoter to that produced from a plasmid containing *gfp* without a promoter was determined. The ratio of the sample without addition of RpoE and BQ10970 was set to 1 for comparison. Error bars indicate standard errors of the means. *, $P < 0.05$ (Student's *t* test).

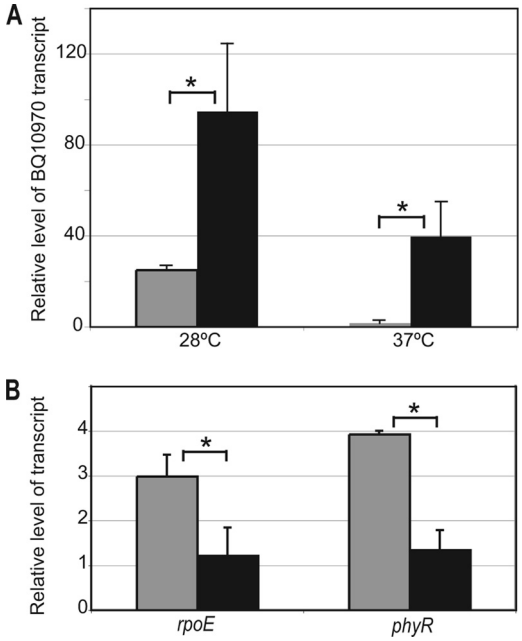

FIG 7 The *B. quintana nepR** mutant strain overexpresses BQ10970 (*nepR*) and has decreased *rpoE* and *phyR* expression. (A) The relative BQ10970 transcript levels in wild-type *B. quintana* (gray) and a *B. quintana* mutant that overexpresses BQ10970 (black) grown at 28 or 37°C was determined by RT-qPCR. (B) The *rpoE* or *phyR* transcript levels produced in wild-type *B. quintana* (gray) and *B. quintana* that contained a plasmid expressing BQ10970 under the control of a constitutively active promoter (black) were determined by RT-qPCR. Bacteria grown at 28°C on chocolate agar plates were used for the analysis. Transcript levels were normalized to the *B. quintana purA* reference gene. Error bars indicate standard errors of the means. *, $P < 0.05$ (Student's *t* test).

in *B. quintana* (Fig. 7A), the transcription of *rpoE* and *phyR* was significantly decreased ($P < 0.05$) (Fig. 7B). From these *in vitro* and *in vivo* experiments, we concluded that BQ10970 inhibits RpoE function and thus functions as an anti-sigma factor. Because of the observed functional and genomic similarities of *B. quintana* BQ10970 and the *Methylobacterium* anti-sigma factor NepR (38), we named the protein BQ10970 NepR.

RpoE function is positively regulated by the response regulator PhyR. Directly downstream of the RpoE operon is the PhyR operon. In other alphaproteobacteria, PhyR functions as an anti-anti-sigma factor by disrupting the interaction between the ECF sigma factor and the anti-sigma factor NepR (31–33, 38). PhyR function is phosphorylation dependent (33, 38). To test for a similar function of *B. quintana* PhyR, we constructed an *E. coli* strain expressing MBP-tagged *B. quintana* PhyR for use in interaction assays. Phosphorylation-dependent disruption of the RpoE-NepR interaction by *B. quintana* PhyR was analyzed with purified recombinant proteins. Addition of MBP-PhyR inhibited the binding interaction between 6×His-RpoE and MBP-NepR only when the PhyR protein was phosphorylated by the addition of acetyl phosphate (Fig. 8). From these data, we concluded that *B. quintana* PhyR functions as an anti-anti-sigma factor in a phosphorylation-dependent manner.

***B. quintana* RpoE confers increased tolerance to high hemin concentrations.** In initial experiments, we determined that *rpoE* transcription is increased when *B. quintana* is grown at a temperature that corresponds to the hemin-rich body louse vector niche, compared to the temperature that corresponds to the hemin-depleted human bloodstream (Fig. 2A). *rpoE* transcription also was upregulated when bacteria were exposed to high concentrations of hemin (Fig. 2B). These observations led us to hypothesize that RpoE-mediated transcription is important for bacterial adaptation and survival within the hemin-toxic body louse gut. To test this hypothesis, we used the isogenic *B. quintana* Δ*rpoE* Δ*nepR* mutant strain. We first tested the Δ*rpoE* Δ*nepR* mutant strain for a growth defect at 37 and 28°C by plating serial dilutions of the Δ*rpoE* Δ*nepR* mutant strain and the wild-type strain on chocolate agar plates. No growth defect of the Δ*rpoE* Δ*nepR* mutant strain was observed at either temperature on chocolate agar (Fig. 9).

The role of RpoE in *B. quintana* tolerance to a high-hemin environment was evaluated by plating *B. quintana* strains on plates with minimal medium agar lacking hemin; this agar does not support *B. quintana* growth. A suspension of wild-type or Δ*rpoE* Δ*nepR* mutant *B. quintana* was spread evenly over the surfaces of separate minimal medium agar plates. Then hemin, an essential iron source for *B. quintana*, was supplied by placing hemin-saturated disks on the *B. quintana*-inoculated agar. The hemin from each disk diffuses on the surface of the agar, establishing a hemin concentration gradient and rescuing bacterial growth when the hemin reaches a concentration sufficient to support *B. quintana* growth. As hemin continues to diffuse into the agar, the zone immediately around the disk gradually achieves higher concentrations of hemin, and if a *B. quintana* strain is more sensitive to these higher concentrations of hemin, growth will be abolished in this zone closest to the disk. This assay permits testing for inhi-

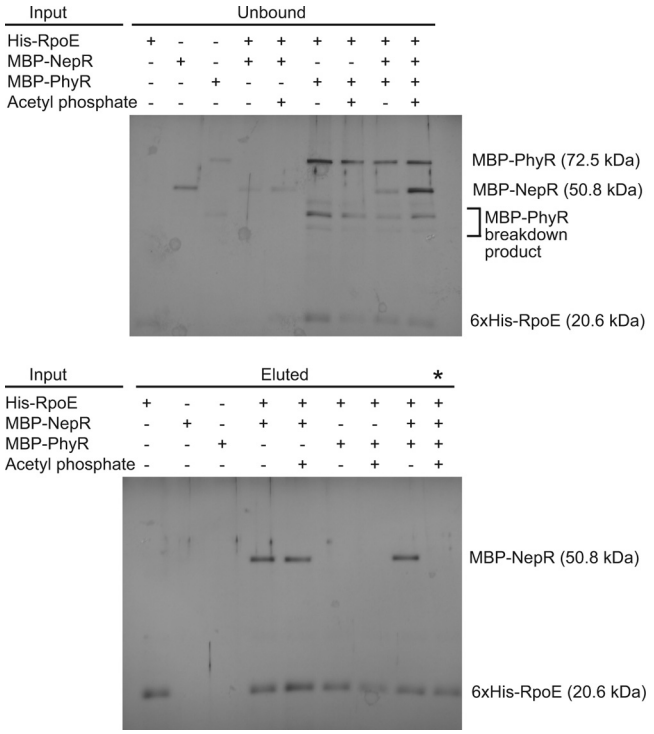

FIG 8 Phosphorylated BQ10980 (PhyR) disrupts the interaction between RpoE and NepR. Purified 6×His-RpoE (250 pmol) was incubated with 500 pmol of purified MBP-NepR with or without 500 pmol of purified MBP-PhyR. In the indicated reaction mixtures, MBP-PhyR was phosphorylated by the addition of acetyl phosphate. The protein mixture was applied to Ni-nitrilotriacetic acid resin and washed to remove unbound proteins, and 6×His-RpoE and any interacting proteins were eluted with Novagen Elute buffer. The unbound (top panel) and eluted (bottom panel) proteins were separated by SDS-PAGE and then silver stained. When phosphorylated MBP-PhyR was present, MBP-NepR no longer coeluted with 6×His-RpoE (the lane is marked by an asterisk). The molecular mass of each protein is in parentheses.

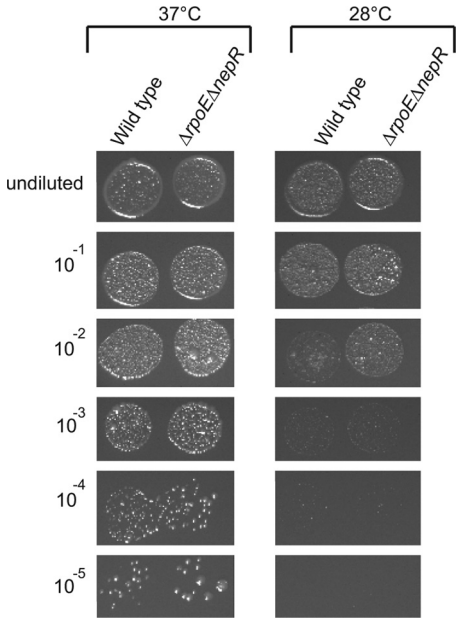

FIG 9 Wild-type *B. quintana* and the Δ*rpoE* Δ*nepR* mutant strain display similar growth on chocolate agar. Wild-type and Δ*rpoE* Δ*nepR* mutant bacteria grown at 37 or 28°C were harvested into M199S medium and adjusted to an OD_{600} of 1. Serial dilutions of the *B. quintana* suspensions were made, and 8 μl of the bacterial suspension was spotted onto chocolate agar plates. The plates were grown for 7 days at 37°C or 14 days at 28°C.

bition of growth due to high hemin concentrations in different *B. quintana* mutants, by testing for the appearance of a zone of growth inhibition when toxic hemin concentrations accumulate immediately surrounding the disk. Minimal medium is used for this analysis because it allows a direct correlation between the bacterial growth observed and the hemin concentration provided from the disk. The plates were incubated at 37°C (for 7 days) or 28°C (for 21 days). At both temperatures, the growth of the wild-type strain was not inhibited by 10 mM hemin and no zone of growth inhibition was observed around the hemin-impregnated disk (Table 2). At 37°C, the Δ*rpoE* Δ*nepR* mutant strain displayed a decreased ability to tolerate high hemin concentrations, and a zone of growth inhibition was observed around the hemin-impregnated disk (Table 2). At 28°C, the Δ*rpoE* Δ*nepR* mutant strain grew very poorly on the minimal medium agar, with few or no colonies observed. These results demonstrated that RpoE- and/or NepR-mediated transcription is necessary for *B. quintana* adaptation to growth in high-hemin environments and that this requirement is greater at 28°C (body louse temperature).

A second method also was used to analyze the hemin sensitivity of the Δ*rpoE* Δ*nepR* mutant strain. Wild-type or Δ*rpoE* Δ*nepR* mutant *B. quintana* harvested from chocolate agar plates was cultivated in M199S liquid medium containing 0, 1, 5, or 10 mM hemin and grown for 24 h at 37 or 28°C. The ability of each strain to tolerate exposure to high hemin concentrations was evaluated by determining the percentage of *B. quintana* that survived following growth in M199S medium supplemented with hemin. At 37°C, the Δ*rpoE* Δ*nepR* mutant strain had a survival defect compared with wild-type *B. quintana* after cultivation in liquid medium supplemented with 5 mM hemin (Fig. 10A). Both the wild-type and Δ*rpoE* Δ*nepR* mutant strains tolerated high hemin concentrations better at 28°C than at 37°C (Fig. 10). At 28°C, the Δ*rpoE* Δ*nepR* mutant strain was significantly more sensitive than the wild-type strain to all three of the hemin concentrations tested (Fig. 10B). From these experiments, we concluded that the deletion of *rpoE* and *nepR* decreases the ability of *B. quintana* to survive exposure to high concentrations of hemin in liquid medium.

The *B. quintana* Δ*rpoE* Δ*nepR* mutant strain has a greater hemin binding capacity than the wild-type strain. The decreased ability of the Δ*rpoE* Δ*nepR* mutant strain to tolerate high concentrations of hemin could be due to increased binding of potentially toxic hemin. To test this, we evaluated the hemin binding capacities of both the wild-type and Δ*rpoE* Δ*nepR* mutant strains at both 28 and 37°C (Table 3). A saturation plot for hemin binding

TABLE 2 Inhibition of *B. quintana* growth by 10 mM hemin

Strain	Temp (°C)	Growth inhibition zone (mm)[a]
Wild type	37	0 ± 0
Δ*rpoE* Δ*nepR* mutant	37	7.17 ± 0.25[b]
Wild type	28	0 ± 0
Δ*rpoE* Δ*nepR* mutant	28	No measurable growth on plate

[a] The distance from the edge of the hemin-saturated disc to the start of bacterial growth was measured.
[b] $P = 0.001$ (Student's *t* test) compared to the wild type.

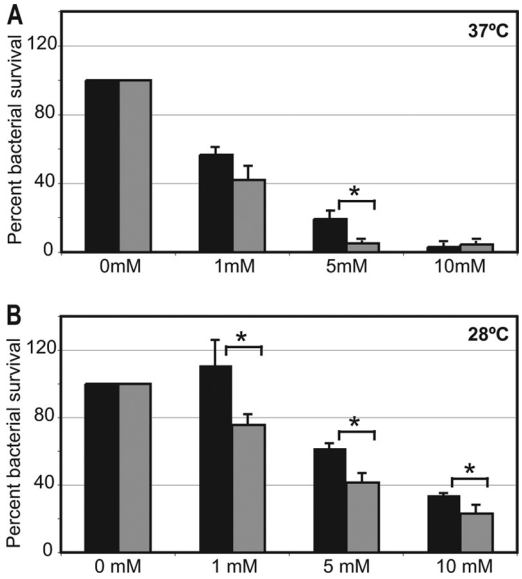

FIG 10 The *B. quintana* Δ*rpoE* Δ*nepR* mutant strain demonstrates increased sensitivity to high hemin concentrations. Wild-type (black) and Δ*rpoE* Δ*nepR* mutant (gray) bacteria were incubated in M199S medium supplemented with hemin at a final concentration of 0, 1, 5, or 10 mM for 24 h at 37°C (A) or 28°C (B). Serial dilutions of the bacterial suspensions were plated to enumerate the *B. quintana* bacteria that survived the 24 h of incubation. Percent survival was calculated as the number of *B. quintana* bacteria that survived in a given concentration of hemin divided by the number of bacteria in the control M199S medium without the addition of supplemental hemin (0 mM). Error bars indicate standard errors of the means. *, $P < 0.05$ (Student's *t* test).

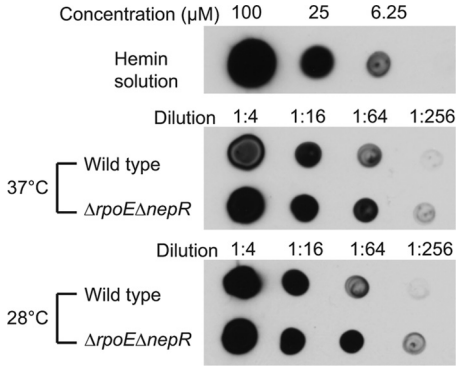

FIG 11 More hemin is associated with *B. quintana* Δ*rpoE* Δ*nepR* mutant bacteria than with wild-type bacteria. Wild-type and Δ*rpoE* Δ*nepR* mutant bacteria were incubated with 1 mM hemin for 1 h at 37 or 28°C. The bacteria were then lysed and spotted onto a nitrocellulose membrane. The amount of hemin present was visualized by exposure to a luminol-based chemiluminescence reagent. Dilutions of hemin solution were analyzed as controls (top panel). The data shown are from one representative experiment.

was generated. Transformation of the data produced a linear plot, indicating that a single class of binding site was present (52–55). The hemin binding data were subjected to nonlinear regression analysis to calculate the K_a and B_{max} of the *B. quintana* strains for hemin (52, 54, 55). The K_a of the Δ*rpoE* Δ*nepR* mutant strain was greater than that of the wild-type strain at both 37 and 28°C (Table 3). The B_{max} of the Δ*rpoE* Δ*nepR* mutant strain was greater than that of the wild-type strain at both 37 and 28°C; however, this difference was statistically significant only at 37°C (Table 3). From this analysis, we concluded that the Δ*rpoE* Δ*nepR* mutant strain is able to bind greater amounts of hemin than wild-type *B. quintana*.

Finally, the amount of hemin bound by each strain also was visualized by exploiting the natural electro-generated chemiluminescent (ECL) behavior of hemin (56, 57). The *B. quintana* wild-type and Δ*rpoE* Δ*nepR* mutant strains were incubated in medium containing 1 mM hemin for 1 h at 37 or 28°C. The bacteria were then washed, pelleted, and lysed. Dilutions of each strain were spotted onto nitrocellulose and visualized with a commercial ECL reagent. Similar to horseradish peroxidase, hemin serves as a catalyst in the chemiluminescence reaction between luminol and H_2O_2 (56, 57). The light produced was visualized by exposing film to the nitrocellulose. At both 37 and 28°C, more light was produced by the Δ*rpoE* Δ*nepR* mutant strain than by wild-type bacteria, indicating that a greater concentration of hemin was associated with the Δ*rpoE* Δ*nepR* mutant strain (Fig. 11). This increased hemin binding capacity and accumulation of hemin in the Δ*rpoE* Δ*nepR* mutant strain could contribute to the increased hemin sensitivity of this strain.

TABLE 3 The Δ*rpoE* Δ*nepR* mutant strain demonstrates increased hemin binding at 37 and 28°C

Strain	Temp (°C)	K_a (μM)	B_{max} (μM)
Wild type	37	25.2 ± 5.9	8.6 ± 1.1
Δ*rpoE* Δ*nepR* mutant	37	43.4 ± 4.2[a]	12.6 ± 0.5[a]
Wild type	28	32.5 ± 9.1	11.3 ± 1.1
Δ*rpoE* Δ*nepR* mutant	28	63.9 ± 11.0[a]	18.3 ± 4.2

[a] $P < 0.05$ (Student's *t* test) compared to wild-type *B. quintana* analyzed at the same temperature.

DISCUSSION

The ECF sigma factors in the ECF15 family are found only in alphaproteobacteria, and they are believed to be responsible for the GSR in this class of organisms (28). To date, detailed functional and structural analyses of ECF15 sigma factors have been performed exclusively with nonhuman pathogens (31–38, 51, 58). We present the first analysis of an ECF15 sigma factor in a human pathogen, *B. quintana*. We first identified the genomic components and functional interactions of the *B. quintana* ECF15 transcription regulatory system, *rpoE* (BQ10960; functions as a sigma factor), *nepR* (BQ10970; functions as an anti-sigma factor), and *phyR* (BQ10980; functions as an anti-anti-sigma factor). The subsequent focus of this study was to characterize the unique role of RpoE in two conditions encountered during *B. quintana* colonization of its human body louse vector: a decreased temperature and an increased hemin concentration. Specific environmental conditions under which ECF15 sigma factor-directed transcription has been demonstrated to be important for bacterial survival include heat, hyperosmotic conditions, nutrient deprivation, desiccation, and UV exposure (31, 33, 35, 37, 38, 51). For *B. quintana*, we determined that the transcription of the ECF15 sigma factor RpoE is increased in response to two stressors present in the body louse vector, a toxic hemin concentration and a decreased temperature. Additionally, we observed decreased survival of *B. quintana* bacteria lacking RpoE-directed transcription following exposure to toxic hemin concentrations (Fig. 10). Our data suggest that *B. quintana* employs the alphaproteobacteria GSR system to survive the unique stressors present in the body louse vector.

B. quintana RpoE is the first ECF15 sigma factor implicated in

hemin tolerance. Non-ECF15 sigma factors from other Gram-negative bacteria are involved in iron sensing, acquisition, and metabolism. Examples of non-ECF15 sigma factors involved in iron sensing include *E. coli* FecI (59), *Pseudomonas aeruginosa* PvdS (60), *Pseudomonas putida* PupI (61), *Bordetella avium* RhuI (62), and *Bordetella pertussis* HurI (63). Activation of transcription directed by these ECF sigma factors involves an iron-sensing outer membrane protein that transmits a signal to an inner membrane protein, which then interacts with the cytoplasmic sigma factor (26). *Bartonella* RpoE and its regulators NepR and PhyR are predicted to be cytoplasmic on the basis of sequence analysis. *B. quintana* produces two putative histidine kinases (BQ10950 and BQ10990) in genomic proximity to *phyR* that could function to phosphorylate PhyR and activate the anti-anti-sigma factor function. Localization algorithms predict that one of these kinases is localized to the cytosol and the other is localized to the periplasm. Both of these putative *B. quintana* histidine kinases are structurally similar to *Caulobacter* PhyK, which phosphorylates PhyR (35). It is possible that one or both of these *B. quintana* kinases are phosphorylated in response to an outer membrane or cytoplasmic iron-sensing protein. Alternatively, these *B. quintana* kinases could directly sense hemin and autophosphorylate in response to changes in iron levels, as occurs with the sensor kinase ChrS of *Corynebacterium diphtheriae* (64).

Because we observed that the transcription of *rpoE* is induced by high concentrations of hemin (Fig. 2), we sought to determine if the Δ*rpoE* Δ*nepR* mutant strain displays perturbed sensitivity to high concentrations of hemin. The concentration of free hemin in the body louse gut following a blood meal has not been determined. However, it is known that in the adult dog tick (*Dermacentor variabilis*), the concentration of hemin in the arthropod gut lumen ranges from 3 to 12 mM over a period of 1 to 43 days after tick detachment from the mammalian host (65). Thus, the concentrations chosen for our hemin sensitivity assays (1, 5, and 10 mM) should encompass the range of hemin concentrations to which *B. quintana* is exposed in the body louse vector. The liquid culture-based hemin sensitivity assay we used in this study has previously been used to quantify the sensitivity of *Bartonella henselae* to hemin (21). Similar to the findings of Roden et al. for *B. henselae*, we observed significantly greater *B. quintana* survival in the presence of a high hemin concentration at 28°C than at 37°C (Fig. 10). In contrast, we found that wild-type *B. quintana* has greater tolerance of high levels of hemin than what was observed previously for *B. henselae*. The difference in hemin sensitivity between the two *Bartonella* species was most prominent at 28°C. The percent survival of *B. quintana* following exposure to 5 mM hemin at 28°C was 62% (Fig. 10), but that of *B. henselae* was less than 1% (21). This difference in hemin tolerance could be an evolutionary adaptation that allows each *Bartonella* species to adapt to its cognate arthropod vector. The vector for *B. henselae* is the cat flea, and the vector for *B. quintana* is the body louse. The cat flea can survive for long periods of time without a blood meal, and fleas do not always remain associated with the host after feeding (66). However, body lice live near the skin on the inner part of the host's clothing and typically require several blood meals per day (67). This vector feeding pattern results in persistently higher concentrations of hemin in the gastrointestinal tract of the body louse than in that of the cat flea; thus, *B. quintana* is required to withstand higher concentrations of hemin than *B. henselae* during vector colonization.

To explore potential mechanisms leading to the increased hemin sensitivity of the Δ*rpoE* Δ*nepR* mutant strain (Table 2; Fig. 10), bacterial hemin binding was analyzed. The Δ*rpoE* Δ*nepR* mutant strain had greater maximal hemin binding than wild-type *B. quintana* (Table 3). Additionally, we observed an increased amount of hemin associated with the Δ*rpoE* Δ*nepR* mutant strain at both 37 and 28°C (Fig. 11). The increased hemin binding by the Δ*rpoE* Δ*nepR* mutant strain could directly contribute to the increased hemin sensitivity of this strain. Other potential mechanisms that could result in increased hemin sensitivity include increased sequestration or decreased hemin export or degradation. It is also possible that RpoE indirectly affects the transcription of one or more of the five *B. quintana hbp* genes and/or the *hut* locus. The Hbp bind hemin (68) and are directly transcriptionally regulated by Irr and RirA transcription factors (69). Components of the *hut* locus are hemin responsive and also are primarily transcriptionally regulated by Irr (20). Future studies of the RpoE regulon will increase our understanding of hemin-regulatory and hemin-responsive networks in *B. quintana*.

In analyzing the functional importance of *B. quintana* RpoE, we determined that the deletion of *rpoE* alone is lethal to *B. quintana* but the simultaneous deletion of *rpoE* and the anti-sigma factor gene *nepR* produces viable bacteria. We also were unable to delete *nepR* alone from *B. quintana*. Similarly, in *Sinorhizobium meliloti*, the deletion of *nepR* alone (smc01505) is lethal (51). *Sinorhizobium nepR* can be disrupted only in the absence of its cognate sigma factor, *rpoE2* (51). In both *Sinorhizobium* and *B. quintana*, *nepR* and *rpoE*/*rpoE2* are cotranscribed and *nepR* directly precedes the sigma factor gene in the operon (51). Interestingly, unlike what we observed in *B. quintana*, in *Sinorhizobium*, deletion of the ECF15 sigma factor gene *rpoE2* alone is not lethal (51). This difference could occur because *Sinorhizobium* encodes six ECF sigma factors that could have redundant functions (70). *B. quintana* has a small, compact 1.5-Mb genome (23) and produces a single ECF sigma factor; thus, it is not surprising that redundant mechanisms for RpoE and NepR function regulation are absent.

All of the *phyR* operons that have been studied have an RpoE-dependent promoter (31, 33, 37), and a second RpoE-independent promoter has been identified in only one alphaproteobacterial genus (37). We identified two distinct promoters for the *B. quintana phyR* operon, only one of which requires RpoE. The *B. quintana* RpoE-responsive promoter contained both −10 and −35 residues that correspond to the canonical motif for ECF15 sigma factors (28). We confirmed the presence of the second, RpoE-independent, promoter by analyzing the transcription of *phyR* in the Δ*rpoE* Δ*nepR* mutant strain (Fig. 4). There also are two promoters for the *phyR* operon in *Sphingomonas*, and similar to the situation in *B. quintana*, one of these promoters functions in the absence of the ECF15 sigma factor (37). In contrast, in *Bradyrhizobium* and *Caulobacter*, the ECF15 sigma factor is essential for the expression of *phyR* (31, 33), which is indicative of a single RpoE-responsive promoter for the *phyR* operon. The *B. quintana* RpoE-independent *phyR* operon TSS promoter elements we identified, −10 CCATAT and −35 TTCATT, lack strong homology to any characterized binding consensus sequence. This RpoE-independent consensus binding sequence and the RpoE binding consensus sequence are both found in the *phyR* promoter region of *B. henselae*, *Bartonella grahamii*, and *Bartonella tribocorum*. This finding suggests that the element that binds this consensus and allows RpoE-independent *phyR* operon transcription is conserved

and functional in all four of these *Bartonella* species. It will be important to study this RpoE-independent *phyR* promoter to identify additional regulatory mechanisms for controlling the expression of the *phyR* operon in *B. quintana*. This likely will provide insight into regulation in *Sphingomonas* and other alphaproteobacteria, as well as in *Bartonella* species.

ECF15 sigma factors were identified relatively recently (30) and orchestrate the alphaproteobacterial GSR. Members of each alphaproteobacterial genus must be able to sense different stressors in their environment to launch the GSR, through PhyR regulation of RpoE. Both of the niches occupied by *B. quintana* are markedly different from the niches/environments occupied by the other alphaproteobacteria whose ECF15 sigma factors have been studied (*Caulobacter*, *Sinorhizobium*, *Bradyrhizobium*, and *Methylobacterium*). The stressors to which the latter genera respond include heat and osmotic stress, starvation for carbon or nitrogen, and desiccation (29). In contrast, *B. quintana* is exposed to alternating shifts in temperature (37 versus 28°C) and changes in ambient hemin concentrations (extremely limited versus toxic). The focus of our study was to evaluate the role of *B. quintana* RpoE in bacterial adaptation to two stressors that are associated with the body louse vector niche. Our work demonstrated that RpoE has a role in conferring the ability of *B. quintana* to tolerate the high hemin concentrations present in the vector gut. Transcriptional modification of hemin uptake and metabolism genes is likely essential for *B. quintana* survival during the transition from the hemin-restricted host bloodstream environment to the hemin-toxic body louse vector environment. Our observation that the Δ*rpoE* Δ*nepR* mutant strain exhibits decreased survival under the high hemin conditions found in the body louse vector suggests that members of the RpoE regulon are important for bacterial survival within the arthropod. Genes within the RpoE regulon likely include additional, vector-specific virulence genes and potential targets for the prevention of transmission to humans. Because vector colonization is essential for the infection of humans with *B. quintana*, targeting of the arthropod vector stage would be ideal for interruption of the body louse-human transmission cycle.

ACKNOWLEDGMENTS

J.E.K. received funding support from a Burroughs Wellcome Fund Clinical Scientist Award in Translational Research, a California HIV Research Program Award, and NIH grant R01AI52813 from the NIAID. S.A. was supported by NIH grant T32A1007641.

REFERENCES

1. **Vinson JW, Varela G, Molina-Pasquel C.** 1969. Trench fever. 3. Induction of clinical disease in volunteers inoculated with *Rickettsia quintana* propagated on blood agar. Am. J. Trop. Med. Hyg. **18**:713–722.
2. **Greub G, Raoult D.** 2004. *Bartonella* infections resurgence in the new century, p 35–68. *In* Fong IW, Drlica K (ed), Emerging infectious diseases of the 21st century, **vol 2**. Springer, New York, NY.
3. **Pulliainen AT, Dehio C.** 2012. Persistence of *Bartonella* spp. stealth pathogens: from subclinical infections to vasoproliferative tumor formation. FEMS Microbiol. Rev. **36**:563–599.
4. **Cockerell CJ, Whitlow MA, Webster GF, Friedman-Kien AE.** 1987. Epithelioid angiomatosis: a distinct vascular disorder in patients with the acquired immunodeficiency syndrome or AIDS-related complex. Lancet **ii**:654–656.
5. **Brouqui P, Lascola B, Roux V, Raoult D.** 1999. Chronic *Bartonella quintana* bacteremia in homeless patients. N. Engl. J. Med. **340**:184–189.
6. **Koehler JE, Sanchez MA, Garrido CS, Whitfeld MJ, Chen FM, Berger TG, Rodriguez-Barradas MC, LeBoit PE, Tappero JW.** 1997. Molecular epidemiology of *Bartonella* infections in patients with bacillary angiomatosis-peliosis. N. Engl. J. Med. **337**:1876–1883.
7. **Bonilla DL, Kabeya H, Henn J, Kramer VL, Kosoy MY.** 2009. *Bartonella quintana* in body lice and head lice from homeless persons, San Francisco, California, USA. Emerg. Infect. Dis. **15**:912–915.
8. **Ito S, Vinson JW.** 1965. Fine structure of *Rickettsia quintana* cultivated in vitro and in the louse. J. Bacteriol. **89**:481–495.
9. **Seki N, Kasai S, Saito N, Komagata O, Mihara M, Sasaki T, Tomita T, Kobayashi M.** 2007. Quantitative analysis of proliferation and excretion of *Bartonella quintana* in body lice, *Pediculus humanus*. Am. J. Trop. Med. Hyg. **77**:562–566.
10. **Wigglesworth VB.** 1941. The sensory physiology of the human louse *Pediculus humanus corporis* de Geer (Anoplura). Parasitology **33**:67–109.
11. **Sander A, Kretzer S, Bredt W, Oberle K, Bereswill S.** 2000. Hemin-dependent growth and hemin binding of *Bartonella henselae*. FEMS Microbiol. Lett. **189**:55–59.
12. **Graça-Souza AV, Maya-Monteiro C, Paiva-Silva GO, Braz GR, Paes MC, Sorgine MH, Oliveira MF, Oliveira PL.** 2006. Adaptations against heme toxicity in blood-feeding arthropods. Insect Biochem. Mol. Biol. **36**:322–335.
13. **Myers WF, Cutler LD, Wisseman CL, Jr.** 1969. Role of erythrocytes and serum in the nutrition of *Rickettsia quintana*. J. Bacteriol. **97**:663–666.
14. **Myers WF, Osterman JV, Wisseman CL, Jr.** 1972. Nutritional studies of *Rickettsia guintana*: nature of the hematin requirement. J. Bacteriol. **109**:89–95.
15. **Stauff DL, Bagaley D, Torres VJ, Joyce R, Anderson KL, Kuechenmeister L, Dunman PM, Skaar EP.** 2008. *Staphylococcus aureus* HrtA is an ATPase required for protection against heme toxicity and prevention of a transcriptional heme stress response. J. Bacteriol. **190**:3588–3596.
16. **Torres VJ, Stauff DL, Pishchany G, Bezbradica JS, Gordy LE, Iturregui J, Anderson KL, Dunman PM, Joyce S, Skaar EP.** 2007. A *Staphylococcus aureus* regulatory system that responds to host heme and modulates virulence. Cell Host Microbe **1**:109–119.
17. **Rasmussen AW, Alexander HL, Perkins-Balding D, Shafer WM, Stojiljkovic I.** 2005. Resistance of *Neisseria meningitidis* to the toxic effects of heme iron and other hydrophobic agents requires expression of *ght*. J. Bacteriol. **187**:5214–5223.
18. **Battisti JM, Sappington KN, Smitherman LS, Parrow NL, Minnick MF.** 2006. Environmental signals generate a differential and coordinated expression of the heme receptor gene family of *Bartonella quintana*. Infect. Immun. **74**:3251–3261.
19. **Liu M, Ferrandez Y, Bouhsira E, Monteil M, Franc M, Boulouis HJ, Biville F.** 2012. Heme binding proteins of *Bartonella henselae* are required when undergoing oxidative stress during cell and flea invasion. PLoS One **7**:e48408. doi:10.1371/journal.pone.0048408.
20. **Parrow NL, Abbott J, Lockwood AR, Battisti JM, Minnick MF.** 2009. Function, regulation, and transcriptional organization of the hemin utilization locus of *Bartonella quintana*. Infect. Immun. **77**:307–316.
21. **Roden JA, Wells DH, Chomel BB, Kasten RW, Koehler JE.** 2012. Hemin binding protein C is found in outer membrane vesicles and protects *Bartonella henselae* against toxic concentrations of hemin. Infect. Immun. **80**:929–942.
22. **Helmann JD.** 1999. Anti-sigma factors. Curr. Opin. Microbiol. **2**:135–141.
23. **Alsmark CM, Frank AC, Karlberg EO, Legault BA, Ardell DH, Canback B, Eriksson AS, Naslund AK, Handley SA, Huvet M, La Scola B, Holmberg M, Andersson SG.** 2004. The louse-borne human pathogen *Bartonella quintana* is a genomic derivative of the zoonotic agent *Bartonella henselae*. Proc. Natl. Acad. Sci. U. S. A. **101**:9716–9721.
24. **Resto-Ruiz SI, Sweger D, Widen RH, Valkov N, Anderson BE.** 2000. Transcriptional activation of the *htrA* (high-temperature requirement A) gene from *Bartonella henselae*. Infect. Immun. **68**:5970–5978.
25. **Helmann JD.** 2002. The extracytoplasmic function (ECF) sigma factors. Adv. Microb. Physiol. **46**:47–110.
26. **Brooks BE, Buchanan SK.** 2008. Signaling mechanisms for activation of extracytoplasmic function (ECF) sigma factors. Biochim. Biophys. Acta **1778**:1930–1945.
27. **Raivio TL, Silhavy TJ.** 2001. Periplasmic stress and ECF sigma factors. Annu. Rev. Microbiol. **55**:591–624.
28. **Starón A, Sofia HJ, Dietrich S, Ulrich LE, Liesegang H, Mascher T.** 2009. The third pillar of bacterial signal transduction: classification of the extracytoplasmic function (ECF) sigma factor protein family. Mol. Microbiol. **74**:557–581.
29. **Starón A, Mascher T.** 2010. General stress response in alphaproteobacteria: PhyR and beyond. Mol. Microbiol. **78**:271–277.

30. **Gourion B, Rossignol M, Vorholt JA.** 2006. A proteomic study of *Methylobacterium extorquens* reveals a response regulator essential for epiphytic growth. Proc. Natl. Acad. Sci. U. S. A. **103**:13186–13191.
31. **Gourion B, Sulser S, Frunzke J, Francez-Charlot A, Stiefel P, Pessi G, Vorholt JA, Fischer HM.** 2009. The PhyR-sigma(EcfG) signalling cascade is involved in stress response and symbiotic efficiency in *Bradyrhizobium japonicum*. Mol. Microbiol. **73**:291–305.
32. **Bastiat B, Sauviac L, Bruand C.** 2010. Dual control of *Sinorhizobium meliloti* RpoE2 sigma factor activity by two PhyR-type two-component response regulators. J. Bacteriol. **192**:2255–2265.
33. **Herrou J, Foreman R, Fiebig A, Crosson S.** 2010. A structural model of anti-anti-sigma inhibition by a two-component receiver domain: the PhyR stress response regulator. Mol. Microbiol. **78**:290–304.
34. **Herrou J, Rotskoff G, Luo Y, Roux B, Crosson S.** 2012. Structural basis of a protein partner switch that regulates the general stress response of alpha-proteobacteria. Proc. Natl. Acad. Sci. U. S. A. **109**:E1415–E1423.
35. **Lourenço RF, Kohler C, Gomes SL.** 2011. A two-component system, an anti-sigma factor and two paralogous ECF sigma factors are involved in the control of general stress response in *Caulobacter crescentus*. Mol. Microbiol. **80**:1598–1612.
36. **Campagne S, Damberger FF, Kaczmarczyk A, Francez-Charlot A, Allain FH, Vorholt JA.** 2012. Structural basis for sigma factor mimicry in the general stress response of Alphaproteobacteria. Proc. Natl. Acad. Sci. U. S. A. **109**:E1405–E1414.
37. **Kaczmarczyk A, Campagne S, Danza F, Metzger LC, Vorholt JA, Francez-Charlot A.** 2011. The PhyR-NepR-σEcfG cascade in *Sphingomonas* sp. Fr1: role in the general stress response and identification of a negative regulator of PhyR. J. Bacteriol. **193**:6629–6638.
38. **Francez-Charlot A, Frunzke J, Reichen C, Ebneter JZ, Gourion B, Vorholt JA.** 2009. Sigma factor mimicry involved in regulation of general stress response. Proc. Natl. Acad. Sci. U. S. A. **106**:3467–3472.
39. **Zhang P, Chomel BB, Schau MK, Goo JS, Droz S, Kelminson KL, George SS, Lerche NW, Koehler JE.** 2004. A family of variably expressed outer-membrane proteins (Vomp) mediates adhesion and autoaggregation in *Bartonella quintana*. Proc. Natl. Acad. Sci. U. S. A. **101**:13630–13635.
40. **Koehler JE, Quinn FD, Berger TG, LeBoit PE, Tappero JW.** 1992. Isolation of *Rochalimaea* species from cutaneous and osseous lesions of bacillary angiomatosis. N. Engl. J. Med. **327**:1625–1631.
41. **Gaynor EC, Cawthraw S, Manning G, MacKichan JK, Falkow S, Newell DG.** 2004. The genome-sequenced variant of *Campylobacter jejuni* NCTC 11168 and the original clonal clinical isolate differ markedly in colonization, gene expression, and virulence-associated phenotypes. J. Bacteriol. **186**:503–517.
42. **Frohman MA, Dush MK, Martin GR.** 1988. Rapid production of full-length cDNAs from rare transcripts: amplification using a single gene-specific oligonucleotide primer. Proc. Natl. Acad. Sci. U. S. A. **85**:8998–9002.
43. **Lee AK, Falkow S.** 1998. Constitutive and inducible green fluorescent protein expression in *Bartonella henselae*. Infect. Immun. **66**:3964–3967.
44. **Hefty PS, Stephens RS.** 2007. Chlamydial type III secretion system is encoded on ten operons preceded by sigma 70-like promoter elements. J. Bacteriol. **189**:198–206.
45. **Kang JG, Hahn MY, Ishihama A, Roe JH.** 1997. Identification of sigma factors for growth phase-related promoter selectivity of RNA polymerases from *Streptomyces coelicolor* A3(2). Nucleic Acids Res. **25**:2566–2573.
46. **MacKichan JK, Gerns HL, Chen YT, Zhang P, Koehler JE.** 2008. A SacB mutagenesis strategy reveals that the *Bartonella quintana* variably expressed outer membrane proteins are required for bloodstream infection of the host. Infect. Immun. **76**:788–795.
47. **Da Re SS, Deville-Bonne D, Tolstykh T, Véron M, Stock JB.** 1999. Kinetics of CheY phosphorylation by small molecule phosphodonors. FEBS Lett. **457**:323–326.
48. **Windholz M.** 1976. The Merck index: an encyclopedia of chemicals, drugs, and biologicals, 9th ed. Merck & Co., Rahway, NJ.
49. **Minnick MF, Sappington KN, Smitherman LS, Andersson SG, Karlberg O, Carroll JA.** 2003. Five-member gene family of *Bartonella quintana*. Infect. Immun. **71**:814–821.
50. **Paiva-Silva GO, Cruz-Oliveira C, Nakayasu ES, Maya-Monteiro CM, Dunkov BC, Masuda H, Almeida IC, Oliveira PL.** 2006. A heme-degradation pathway in a blood-sucking insect. Proc. Natl. Acad. Sci. U. S. A. **103**:8030–8035.
51. **Sauviac L, Philippe H, Phok K, Bruand C.** 2007. An extracytoplasmic function sigma factor acts as a general stress response regulator in *Sinorhizobium meliloti*. J. Bacteriol. **189**:4204–4216.
52. **Amano A, Kuboniwa M, Kataoka K, Tazaki K, Inoshita E, Nagata H, Tamagawa H, Shizukuishi S.** 1995. Binding of hemoglobin by *Porphyromonas gingivalis*. FEMS Microbiol. Lett. **134**:63–67.
53. **Rosenthal HE.** 1967. A graphic method for the determination and presentation of binding parameters in a complex system. Anal. Biochem. **20**:525–532.
54. **Smalley JW, Birss AJ, McKee AS, Marsh PD.** 1998. Hemin regulation of hemoglobin binding by *Porphyromonas gingivalis*. Curr. Microbiol. **36**: 102–106.
55. **Tompkins GR, Wood DP, Birchmeier KR.** 1997. Detection and comparison of specific hemin binding by *Porphyromonas gingivalis* and *Prevotella intermedia*. J. Bacteriol. **179**:620–626.
56. **Chen GN, Zhang L, Lin RE, Yang ZC, Duan JP, Chen HQ, Hibbert DB.** 2000. The electrogenerated chemiluminescent behavior of hemin and its catalytic activity for the electrogenerated chemiluminescence of lucigenin. Talanta **50**:1275–1281.
57. **Ikariyama Y, Suzuki S, Aizawa M.** 1982. Luminescence immunoassay of human serum albumin with hemin as labeling catalyst. Anal. Chem. **54**: 1126–1129.
58. **Gourion B, Francez-Charlot A, Vorholt JA.** 2008. PhyR is involved in the general stress response of *Methylobacterium extorquens* AM1. J. Bacteriol. **190**:1027–1035.
59. **Mahren S, Braun V.** 2003. The FecI extracytoplasmic-function sigma factor of *Escherichia coli* interacts with the beta′ subunit of RNA polymerase. J. Bacteriol. **185**:1796–1802.
60. **Tiburzi F, Imperi F, Visca P.** 2008. Intracellular levels and activity of PvdS, the major iron starvation sigma factor of *Pseudomonas aeruginosa*. Mol. Microbiol. **67**:213–227.
61. **Koster M, van Klompenburg W, Bitter W, Leong J, Weisbeek P.** 1994. Role for the outer membrane ferric siderophore receptor PupB in signal transduction across the bacterial cell envelope. EMBO J. **13**:2805–2813.
62. **Kirby AE, Metzger DJ, Murphy ER, Connell TD.** 2001. Heme utilization in *Bordetella avium* is regulated by RhuI, a heme-responsive extracytoplasmic function sigma factor. Infect. Immun. **69**:6951–6961.
63. **Brickman TJ, Vanderpool CK, Armstrong SK.** 2006. Heme transport contributes to *in vivo* fitness of *Bordetella pertussis* during primary infection in mice. Infect. Immun. **74**:1741–1744.
64. **Ito Y, Nakagawa S, Komagata A, Ikeda-Saito M, Shiro Y, Nakamura H.** 2009. Heme-dependent autophosphorylation of a heme sensor kinase, ChrS, from *Corynebacterium diphtheriae* reconstituted in proteoliposomes. FEBS Lett. **583**:2244–2248.
65. **Tarnowski BI, Coons LB.** 1989. Ultrastructure of the midgut and blood meal digestion in the adult tick *Dermacentor variabilis*. Exp. Appl. Acarol. **6**:263–289.
66. **Rust MK, Dryden MW.** 1997. The biology, ecology, and management of the cat flea. Annu. Rev. Entomol. **42**:451–473.
67. **Kittler R, Kayser M, Stoneking M.** 2003. Molecular evolution of *Pediculus humanus* and the origin of clothing. Curr. Biol. **13**:1414–1417.
68. **Carroll JA, Coleman SA, Smitherman LS, Minnick MF.** 2000. Hemin-binding surface protein from *Bartonella quintana*. Infect. Immun. **68**: 6750–6757.
69. **Battisti JM, Smitherman LS, Sappington KN, Parrow NL, Raghavan R, Minnick MF.** 2007. Transcriptional regulation of the heme binding protein gene family of *Bartonella quintana* is accomplished by a novel promoter element and iron response regulator. Infect. Immun. **75**:4373–4385.
70. **Galibert F, Finan TM, Long SR, Puhler A, Abola P, Ampe F, Barloy-Hubler F, Barnett MJ, Becker A, Boistard P, Bothe G, Boutry M, Bowser L, Buhrmester J, Cadieu E, Capela D, Chain P, Cowie A, Davis RW, Dreano S, Federspiel NA, Fisher RF, Gloux S, Godrie T, Goffeau A, Golding B, Gouzy J, Gurjal M, Hernandez-Lucas I, Hong A, Huizar L, Hyman RW, Jones T, Kahn D, Kahn ML, Kalman S, Keating DH, Kiss E, Komp C, Lelaure V, Masuy D, Palm C, Peck MC, Pohl TM, Portetelle D, Purnelle B, Ramsperger U, Surzycki R, Thebault P, Vandenbol M, Vorholter FJ, Weidner S, Wells DH, Wong K, Yeh KC, Batut J.** 2001. The composite genome of the legume symbiont *Sinorhizobium meliloti*. Science **293**:668–672.
71. **Simon R, Priefer U, Puhler A.** 1983. A broad host range mobilization system for in vivo genetic engineering: transposon mutagenesis in Gram negative bacteria. Nat. Biotechnol. **1**:784–791.